Charge ordering and charge dynamics in $Nd_{2-x}Sr_xNiO_4$ ($0.33 \leqslant x \leqslant 0.7$)

K. Ishizaka and Y. Taguchi*
Department of Applied Physics, University of Tokyo, Bunkyo-ku, Tokyo 113-8656, Japan

R. Kajimoto
Department of Physics, Ochanomizu University, Bunkyo-ku, Tokyo 112-8610, Japan

H. Yoshizawa
Neutron Scattering Laboratory, ISSP, University of Tokyo, Tokai, Ibaraki 319-1106, Japan

Y. Tokura
Department of Applied Physics, University of Tokyo, Bunkyo-ku, Tokyo 113-8656, Japan
and Correlated Electron Research Center (CERC), AIST, Tsukuba, Ibaraki 305-0046, Japan
(Received 30 November 2002; published 27 May 2003)

Charge ordering phenomena and their effects on charge dynamics have been investigated for single crystals of $R_{2-x}Sr_xNiO_4$ (R=La, Nd) with $x=0.5$ for R=La and $0.33 \leqslant x \leqslant 0.70$ for R=Nd by measurements of neutron diffraction and optical reflectivity spectra. The essential features of charge dynamics for $0.33 \leqslant x \leqslant 0.5$ appear to be least affected by R species (La or Nd). In $x \geqslant 0.5$, commensurate checkerboard (CB)-type charge order shows up at such a high temperature as $T_{CO}^{C} \sim 480$ K. An incommensurate stripe order, that tends to take over the CB-type charge order at lower temperatures, is also clearly observed up to $x=0.7$. The remarkable evolution of the pseudogap feature as lowering temperature is observed in the optical conductivity spectrum. As x is increased, the energy scale (Δ_{PG}), the onset T (T_{PG}) of the pseudogap, and the in-plane resistivity upturn T ($T_{\rho_{ab}}$) scale with each other and decrease monotonically after taking a maximum at $x=0.5$, as T_{CO}^{C} is simultaneously reduced. The results indicate that the charge dynamics is significantly regulated by emergence of the CB-type charge correlation, and that the melting of the CB-type charge order must be playing a key role in driving the insulator-metal transition at $x \sim 0.9$.

DOI: 10.1103/PhysRevB.67.184418 PACS number(s): 75.30.Fv, 71.27.+a, 71.45.Lr, 78.20.−e

I. INTRODUCTION

Spin/charge ordering and related charge dynamics have been important topics in a broad range of materials with strongly correlated electrons.[1] Occasionally the order pattern depends on the filling level of the system, a typical case of which is stripe ordering, as extensively studied in the $La_{2-x}Sr_xCuO_4$ (LSCO) system.[2] In LSCO, that is among a family of high-T_c superconductors, the stripe order changes its direction with hole doping from *diagonal* to *vertical*, almost concomitantly with the insulator-superconductor transition at $x \sim 0.05$.[3] The interrelation among the doping concentration, ordering pattern, and charge dynamics has been widely investigated both experimentally and theoretically. The $La_{2-x}Sr_xNiO_4$ (LSNO), isostructural with LSCO, is also well known to show a similar type of diagonal stripe ordering in the low-doped region ($0.135 \leqslant x \leqslant 0.5$).[4–9] In contrast to LSCO, the insulating nature of the ground state in LSNO is significantly robust against hole doping, where the insulator-metal (I-M) transition does not occur until $x \sim 0.9$.[10–12] This is possibly due to the higher spin value ($S=1$) and/or the stronger electron-phonon coupling. However, partly due to the difficulty in preparing single crystal specimens, the material phase in such a high-doped region ($x>0.5$) close to the I-M transition has remained to be explored.

The stripe order in LSNO with $x \leqslant 0.5$ is characterized by an incommensurability ϵ, with which the superlattice modulation vectors of charge and spin are given as $\vec{g}_{charge} = (2\epsilon, 0, 0)$ and $\vec{g}_{spin} = (1-\epsilon, 0, 0)$ in the orthorhombic setting, respectively. In this x region, ϵ is approximately equal to the hole concentration x,[9] as is characteristic of stripe order. The stripe order is most stabilized at $x=\epsilon=1/3$ where the modulation vectors of the charge and spin become equivalent. The incommensurate charge ordering transition at $T_{CO}^{IC} \sim 240$ K is detected as anomalies of transport, optical, and thermal properties in various kinds of measurements.[13–15] At $x=1/2$, which is another fixed point for commensurability, a rather complicated ordering process has been observed in a recent neutron diffraction measurement.[16] First, a commensurate checkerboard (CB)-type charge order is observed to evolve below $T_{CO}^{C} \sim 480$ K, which is eventually taken over by, while coexisting with, an incommensurate ($\epsilon \sim 0.44$) stripe order with lowering temperature below $T_{CO}^{IC} \sim 180$ K. The low-T stripe order seems to subsist from the lower doped region with changing its ϵ value. Thus, the anomaly specific to $x=1/2$ shows up as the stabilization of higher-T scale CB-type order, which is distinct from the stripe in origin. In this study, we have performed measurements of neutron diffraction and optical conductivity spectra in $R_{2-x}Sr_xNiO_4$ (R=Nd) system, for which large single crystals are available over a wider x region ($0.33 \leqslant x \leqslant 0.7$ so far) (Ref. 17), than in the R=La case (up to $x=0.5$). The purpose of this paper is to clarify the ordering phenomena in a higher-doped region of $x>0.5$ to

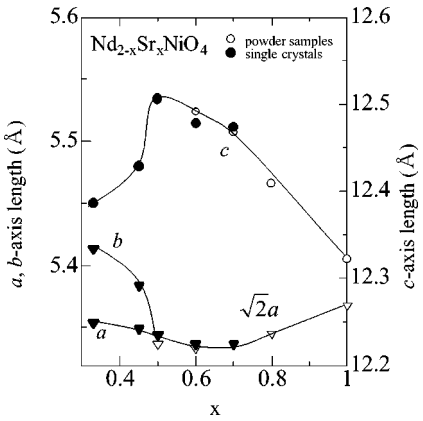

FIG. 1. Room-temperature lattice parameters for $Nd_{2-x}Sr_xNiO_4$ (NSNO) system. The crystal structure at room temperature is low temperature orthorhombic (LTO) in $x \leqslant 0.45$ and high temperature tetragonal (HTT) in $x \geqslant 0.50$. Solid lines are merely the guide to the eyes.

make comparison with the low-doped region, and to investigate how they influence the charge dynamics, especially when the system approaches the insulator-metal transition.

II. EXPERIMENT

Single crystals of $Nd_{2-x}Sr_xNiO_4$ (NSNO) were grown by a floating-zone method similar to the case of $La_{2-x}Sr_xNiO_4$ (LSNO) crystals.[14] By x-ray powder diffraction measurements, the average crystal structure and symmetry at room temperature were determined to be high-temperature-tetragonal (HTT) $I4/mmm$ for $x \geqslant 0.5$ and low-temperature-orthorhombic (LTO) $Bmab$ for $x \leqslant 0.45$. The lattice parameters at room temperature for NSNO system are plotted in Fig. 1. The LTO phase seems to extend to a higher x region compared to $R=$La compounds, where the LTO phase disappears at $x \approx 0.22$.[5,7] This must be due to the difference in the ionic radius of R. Apart from the structural transition, the x dependence of the lattice parameters resembles that of LSNO,[10] so as the c-axis length takes a local maximum at $x=0.5$. For $x=0.5$, a HTT-LTO phase transition was discerned at around 230 K. For $x \geqslant 0.6$, the HTT-LTO transition no longer exists, at least down to 10 K.

Resistivity was measured along the ab plane by a standard four-probe method. For the optical measurements, the ab plane was cut from the crystal boule, and was polished to the optical flatness with alumina powder. Reflectivity spectra was measured using a Fourier-transform interferometer for a photon energy range of 0.01–0.8 eV and grating spectrometers for 0.6–36 eV. Synchrotron radiation at UVSOR, Institute for Molecular Science, was utilized for the measurements between 6 and 36 eV. The temperature was varied from 10 to 590 K in the measurement between 0.01 and 3 eV. Optical conductivity spectra were obtained by Kramers-Kronig analyses of the reflectivity data at respective temperatures, which were extrapolated with the room-temperature data for the higher-energy region ($\geqslant 3$ eV).

The neutron diffraction measurements were performed using the triple axis spectrometer GPTAS installed at the JRR-3M reactor in JAERI, Tokai, Japan with a fixed incident neutron momentum of $k_i = 3.81$ Å^{-1}. The typical size of sample was 5 mm$\phi \times 25$ mm. We chose a combination of horizontal collimators of 40′-40′-40′-80′ (from the monochromator to the detector), and set two PG filters before the monochromator and after the sample positions to eliminate the higher order contamination. The temperature was varied from 10 to 590 K using a closed-cycle He refrigerator. Although most of the samples have the crystal structure of pseudo-tetragonal ($I4/mmm$) whose unit cell size is described as $a_t \times a_t \times c_t$, we employ an orthorhombic setting with larger unit cell size $\sqrt{2}a_t \times \sqrt{2}a_t \times c_t$ for convenience of easier comparison with the preceding works.

III. RESULTS AND DISCUSSION

A. Charge ordering and charge dynamics in $x=0.5$ for $R=$ La and Nd

In this section, we present the experimental results for the $x=0.5$ RSNO ($R=$La and Nd) and discuss how the charge dynamics is influenced by the charge ordering. The CB-type charge order as well as the incommensurate charge/spin stripe has recently been observed by neutron diffraction in the $x=0.5$ LSNO.[16] In the $x=0.5$ NSNO, the CB-type charge order was unfortunately not able to be discerned by diffraction measurements due to the HTT-LTO lattice-structural transition at ~ 230 K, which allows the strong Bragg peaks of the LTO phase to take over the possible superlattice peaks corresponding to the CB-type charge ordered state. However, the resistivity and optical conductivity data for $R=$La and Nd show a close resemblance as shown later in this section, suggesting that the electronic properties including the CB-type charge ordering are least affected by the R substitution, or the HTT-LTO structural transition.

The temperature (T) dependence of the in-plane resistivity ρ_{ab} for $Nd_{2-x}Sr_xNiO_4$ with $0.33 \leqslant x \leqslant 0.7$ is presented in Fig. 2. At high T, a fairly conductive behavior is observed with $\rho_{ab} \sim 10^{-3}$ Ω cm. For the case of $x=0.33$, there is a steep change in ρ_{ab} at ~ 500 K which is likely due to the HTT-LTO transition. Upon lowering T, the respective ρ_{ab} eventually diverges, indicating the insulating ground state. Among the temperatures, that temperature where ρ_{ab} starts to diverge is the highest in $x=0.5$. This is more apparent the $d(\log\rho)/dT$ vs T curves shown in the inset of Fig. 2: An abrupt decrease of $d(\log\rho)/dT$ below the CB-type charge order transition temperature, $T_{CO}^{C} \sim 480$ K, is observed for $x=0.5$. ρ_{ab} of the $x=0.5$ LSNO (shown by a broken line in Fig. 2) almost coincides with that of the $x=0.5$ NSNO, indicating that the charge dynamics goes almost parallel for the $R=$La and Nd compounds with $x=0.5$. A change in ρ_{ab} upon the charge ordering transition is observed not so clearly as in $x=0.33$, possibly because of the small charge-modulation amplitude of the CB-type order compared to the stripe order in $x=0.33$.

As shown in Fig. 3, the in-plane optical conductivity $\sigma(\omega)$ spectra also show a similar behavior for $R=$La and Nd. Upon lowering temperature from ~ 590 K, a gap structure is gradually formed. At $T > T_{CO}$, however, a fully

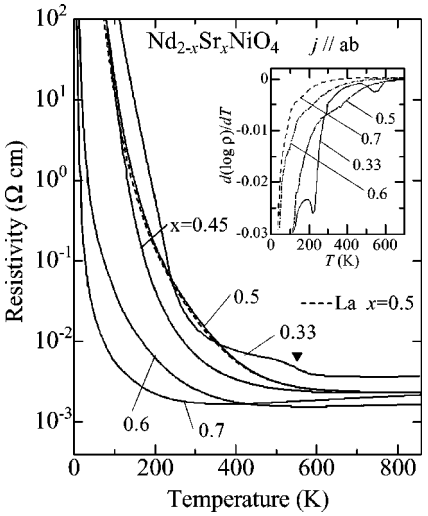

FIG. 2. Temperature dependence of the in-plane resistivity for $Nd_{2-x}Sr_xNiO_4$ (NSNO) with $x=0.33$, 0.45, 0.5, 0.6, and 0.7. A solid triangle on the ρ_{ab} curve of $x=0.33$ denotes the anomaly due to the HTT-LTO structural transition which is not explicitly relevant to charge ordering phenomena. A resistivity curve with a broken line is the data of $La_{2-x}Sr_xNiO_4$ (LSNO, $x=0.5$). The inset shows $d(\log\rho)/dT$ of NSNO for respective x.

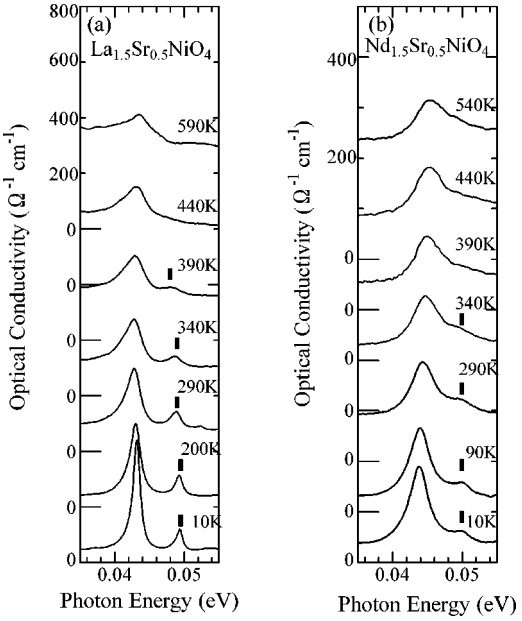

FIG. 4. Temperature dependence of Ni-O bending phonon mode around 0.045 eV in the in-plane $\sigma(\omega)$ spectra of (a) LSNO (R = La), $x=0.5$ and (b) NSNO (R = Nd), $x=0.5$. Solid rectangles show the appearance of a new mode below T_{CO}^{C}.

opened (zero-conductivity) gap is not observed in accord with the fairly conductive value of resistivity. Such a pseudogap (i.e., a gaplike feature with finite conductivity at $\omega\rightarrow 0$) formation indicates that the coherent charge motion is strongly suppressed by a dynamical component of the CB-type charge order from >600 K, far higher than the ordering temperature T_{CO}^{C}. Here we notice that there exists an isosbectic (equal-absorption) point ($\sim$0.57 eV and 0.60 eV for R = La and Nd, respectively) where the spectral weight in the lower energy region is transferred to the higher energy region as decreasing T. Hereafter, we regard the isosbectic point as an energy scale of pseudogap (Δ_{PG}), below which the dynamics of doped holes is strongly damped. When further decreasing T below T_{CO}^{C}, a real gap showing zero conductivity might be anticipated to show up in the low-energy part as the charge order parameter, which gradually shifts the isosbectic point to higher energy. However, a well-defined gap feature in the $\sigma(\omega)$ spectrum is not observed until the temperature is cooled down sufficiently below T_{CO}^{C}. This is partly because the magnitude of the gap is small. In $x=0.5$, the charge gap becomes at most $\sim$0.12 eV at $\sim$150 K [estimated by linearly extrapolating the rising edge of $\sigma(\omega)$; also see Fig. 3], which is much smaller than that ($\sim$0.3 eV) in $x=0.33$ LSNO.[18] In both of the spectra for R = La and Nd, a slight recovery of spectral weight below the isosbectic-point energy is observed below $\sim$150 K. It corresponds to the reduction of the CB-type charge order gap by the formation of a stripe order which competes with the CB-type order. The T-dependent characteristics will be discussed in detail later in this section.

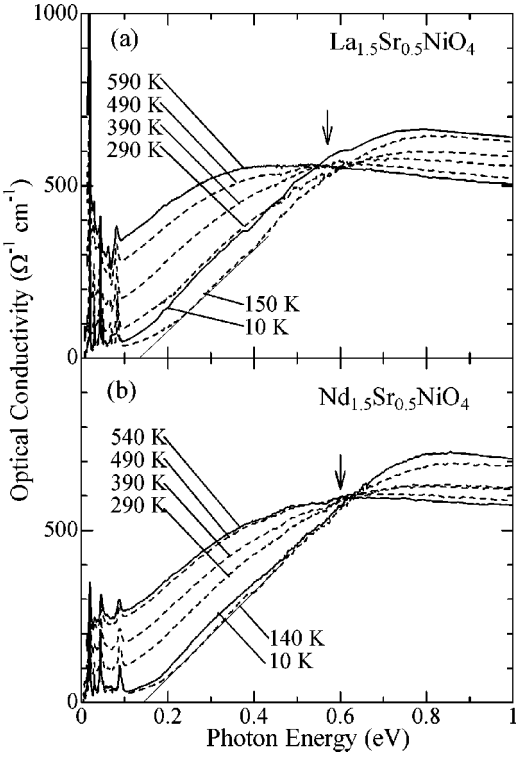

FIG. 3. In-plane optical conductivity spectra $\sigma(\omega)$ of (a) LSNO, $x=0.5$ and (b) NSNO, $x=0.5$ below 1 eV at various temperatures.

A clear anomaly in decreasing T below T_{CO}^{C} is also observed in the infrared phonon spectrum of $\sigma(\omega)$. At high T above 500 K, infrared-active modes expected for the HTT ($I4/mmm$) phase are commonly observed in both spectra for R = La and Nd. However, when lowering T below 400 K, the in-plane Ni-O bending mode at $\sim$0.043 eV starts to split, as shown in Fig. 4. From the T dependence, this anomaly is attributed to the lowering of the crystal structure symmetry

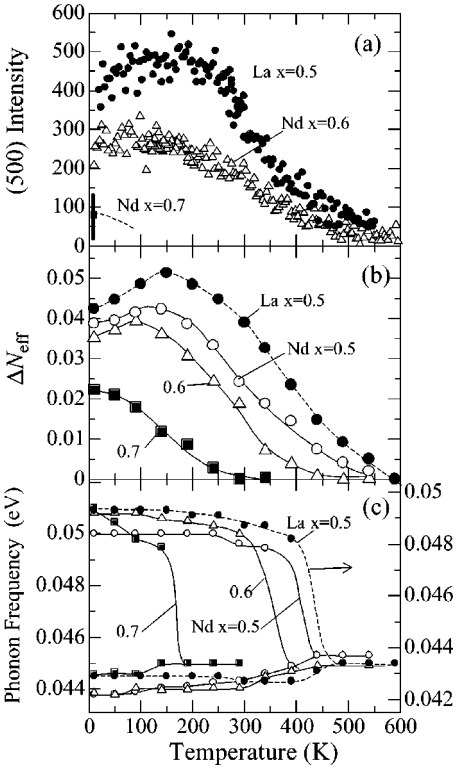

FIG. 5. Temperature dependence of (a) the (5 0 0) neutron-diffraction superlattice peak intensity normalized by a standard Bragg reflection for (R=La, x=0.5) and (R=Nd, x=0.6,0.7), (b) loss of the optical-conductivity spectral intensity due to the pseudogap opening ($\Delta N_{\rm eff}$) for (R=La, x=0.5) and (R=Nd, x=0.5–0.7), and (c) Ni-O bending phonon mode frequency for (R=La, x=0.5) and (R=Nd, x=0.5–0.7).

induced by the charge order formation. A similar anomaly in lattice dynamics was also reported in a Raman scattering study on x=0.5 LSNO,[19] for example as the evolution of a strong breathing mode below $T_{\rm CO}^{\rm C}$ in A_{1g} symmetry. Such phonon anomalies are often observed in typical charge ordering systems, such as Mn oxides, Fe oxides, and x=1/3 LSNO.[1,18,20,21] As noticed in Fig. 4, the mode splitting due to the CB-type order is observed commonly for R=La and Nd. However, the phonon spectral shape for R=La is sharper, perhaps due to the clearer gap opening which gives rise to less dielectric screening of phonons. Incidentally, the effect of the LTO-type tilting distortion which exists below 230 K for x=0.5 NSNO is too small to be discerned in the infrared phonon spectrum.

In Fig. 5, we compare the T variation of several quantities which characterize the CB-type charge order. Figure 5 also includes the results for x=0.6 and 0.7 NSNO (see Sec. III B), yet in this section let us confine ourselves on the results for x=0.5 LSNO and NSNO. The intensity of the superlattice peak (5 0 0) shown in Fig. 5(a) was measured by neutron diffraction in the (h 0 l) zone. To remove the T dependence of the background intensity, the scattering intensity at (4.7 0 0) was also measured and subtracted. The (5 0 0) reflection, which is not allowed in the HTT phase, appears when the unit cell is doubled in size by the CB-type charge order formation. Hence, it can be used as an estimate of the CB-type charge order parameter. With decreasing T, it starts to evolve gradually at such a high T as ~450 K. With a further lowering of T, however, it decreases at ~180 K. This behavior arises from the competition between the commensurate CB-type charge order and the incommensurate stripe order, the latter of which is formed below $T_{\rm CO}^{\rm IC}$~180 K. The in-plane correlation lengths of the CB-type and stripe-type charge orders estimated from the width of the respective superlattice peaks are both ≈20 Å at 10 K, indicating their short-range character. More details on the neutron diffraction measurement for x=0.5 LSNO are described elsewhere.[16] Since the x=0.5 NSNO undergoes a structural transition to the LTO phase at ~230 K, which allows a normal Bragg peak at (5 0 0), the measurement of the CB-type superlattice peak for x=0.5 was only possible for LSNO, as already mentioned. The $\Delta N_{\rm eff}$ shown in Fig. 5(b) is a measure of spectral-weight loss due to the (pseudo-)gap opening. For each T we calculated the spectral weight below the isosbectic point by the effective number of electrons, $N_{\rm eff}(\omega_{\rm c}) = (2m/\pi e^2 N)\int_0^{\omega_{\rm c}}\sigma(\omega')d\omega'$, where m, N, and $\omega_{\rm c}$ represent the free electron mass, the number of Ni atoms per unit volume, and the isosbectic point, respectively. Then we performed the subtraction of $N_{\rm eff}$ for each T from the one at the highest T (e.g., 590 K for R=La) as $\Delta N_{\rm eff}(T) = N_{\rm eff}(590{\rm K}) - N_{\rm eff}(T)$. As for the analysis of phonon anomaly, the frequency of the Ni-O in-plane bending mode which splits below $T_{\rm CO}^{\rm C}$ was estimated by Lorentzian curve fitting and plotted in Fig. 5(c).

It is immediately noticed in Fig. 5 that the CB-type charge order, pseudogap formation, and phonon anomaly are closely related to each other. As the superlattice peak evolves below ~450 K, the Ni-O bending mode shows some redshift followed by the emergence of another mode at slightly lower T, indicating that the phonon anomaly probes the CB-type charge order formation. Note that the pseudogap starts developing already at 590 K. This suggests that the charge dynamics in this system is influenced by the CB-type charge correlation at a sufficiently higher T than $T_{\rm CO}^{\rm C}$. This is also evidenced by the transport data: The resistivity starts increasing from a temperature above 600 K, while the T dependence of $\Delta N_{\rm eff}$ at lower T fairly resembles that of the superlattice peak in Fig. 5(a). The simultaneous reduction of superlattice peak intensity and $\Delta N_{\rm eff}(T)$ is observed below 180 K, as the IC stripe begins to be formed.[22] Thus, $\Delta N_{\rm eff}$ at $T \leqslant T_{\rm CO}^{\rm C}$ reflects the optical gap induced by the CB-type charge order, and the gap due to the stripe appears to be smaller than that of the CB-type order in x=0.5. Also note that quite a common feature is observed even when R is changed from La to Nd, although the magnitude of pseudogap differs slightly (see and compare the isosbectic-point position indicated by arrows in Fig. 3).

From the above results, we conclude that the CB-type charge order in x=0.5 has an anomalously high temperature and energy scale. Nevertheless, the CB-type order seems to be weak in amplitude. Besides the hole itinerancy of the x=0.5 state, this may be partly due to the stacking frustration along the c axis, which is caused by the degeneracy of equivalent stacking directions, i.e., along either [1/2 0 1/2] or

[0 1/2 1/2]. It prevents three-dimensional long range ordering, which makes the CB-type order quasi-two-dimensional and thus diffusive. The origin of incommensurate stripe order, on the other hand, may be attributed to spin-spin interaction as argued in Ref. 16. The spin interaction gives rise to an incommensurate (stripe-type) correlation to gain the exchange energy between the nearest neighbor sites. Thus, as the magnetic correlation gradually evolves in lowering T, the stripe order takes over some part of the CB-type order at T_{CO}^{IC}, and eventually the spin correlation itself also freezes at lower temperature T_{SO}^{IC}.[24] Whether such a coexistence of CB and stripe phases appears as a macroscopic phase separation or microscopic phase mixture could not be determined with the present experimental results alone. It is likely that cooperation and competition among Coulomb interaction, electron-phonon coupling, and spin correlation give rise to such a complex T-dependent ordering phenomenon, as observed.

B. x dependence in $Nd_{2-x}Sr_xNiO_4$ ($0.33 \leqslant x \leqslant 0.7$)

In this section, we discuss the x dependence of the ordering phenomena in the $R=$Nd system, whose single crystalline samples with higher Sr concentration up to $x=0.70$ were available for measurements of optical reflectivity and neutron diffraction. We have observed for $x=0.33$,0.45, and 0.50 that the stripe order temperatures, T_{CO}^{IC} and T_{SO}^{IC}, are close to those in the LSNO system.[16] For $x \geqslant 0.5$, we have found in the present study that the stripe order robustly subsists up to $x=0.7$. The CB-type charge order was also observed, though diffusive, in the $x=0.6$ sample (see Fig. 8 for those transition temperatures). We will discuss these results at the end of this section together with the transport and optical properties.

The resistivity behaviors for $0.33 \leqslant x \leqslant 0.7$ are presented in Fig. 2. The most insulating at low temperature is the $x=0.33$ crystal, in which the resistivity anomaly signals the charge stripe order below $T_{CO}^{IC} \sim 230$ K. The anomaly is more clearly discerned in a plot of $d(\log \rho)/dT$ vs T (the inset of Fig. 2) as the local minimum at around 230 K. The resistivity jump at ~ 550 K can be attributed to the HTT-LTO transition. With increasing x, the resistivity seems to decrease once ($x=0.45$), while it increases again at $x=0.50$ especially in the intermediate T region, due to the emergence of the CB-type charge ordering. With a further increase x over 0.5, the resistivity tends to decrease rapidly in a wide T-region, though it still diverges as $T \rightarrow 0$. The T dependence is also x dependent, as observed in the change of the onset temperature ($T_{\rho_{ab}}$) of the resistivity upturn. $T_{\rho_{ab}}$ obviously takes the maximum (>800 K) at $x=0.5$. It seems to decrease as x is decreased; however, still >700 K for $x=0.45$, and is not properly defined for $x=0.33$ due to the LTO transition [in the LSNO system, $T_{\rho_{ab}}$ is ~ 480 K for $x=0.33$ (Ref. 18)]. For $x>0.5$, on the other hand, $T_{\rho_{ab}}$ decreases to 580 and 380 K at $x=0.6$ and 0.7, respectively. Even a higher doped region (up to $x=1.4$) has recently been explored with use of single crystalline thin films of LSNO, where non-diverging resistivity at the lowest T, i.e., a barely metallic feature, was eventually observed above $x_{M\text{-}I} \sim 0.9$.[11,12]

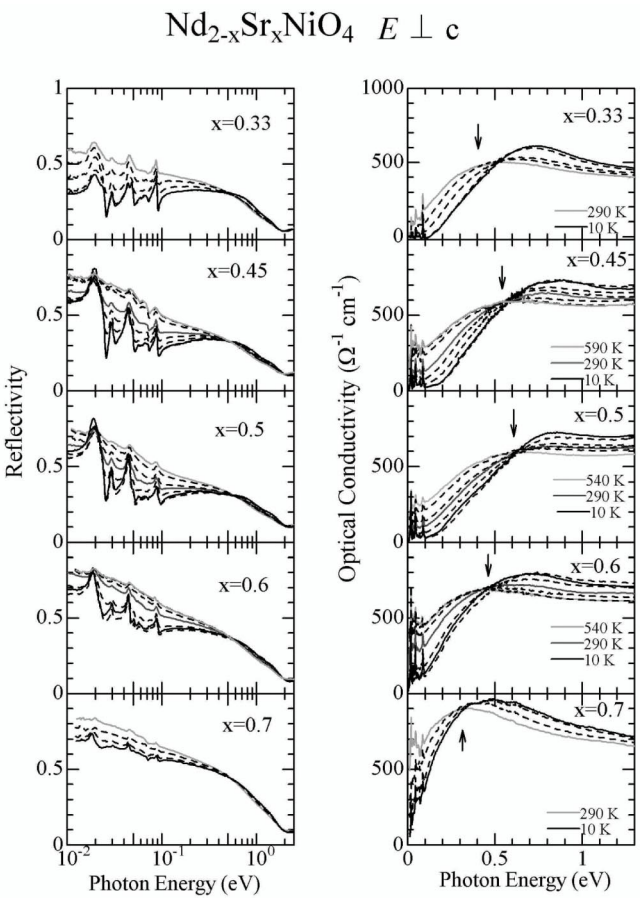

FIG. 6. Temperature dependence of the in-plane (light ***E*** vector $\perp$ ***c***) reflectivity (left side) and optical conductivity (right side) spectra for $Nd_{2-x}Sr_xNiO_4$ with $x=0.33$, 0.45, 0.5, 0.6, and 0.7. The respective spectra are shown at temperatures of every 100 K between the indicated ones (see the text for details).

Now let us move on to the x variation of the optical conductivity spectrum $\sigma(\omega)$, as shown in Fig. 6. Figure 6 shows the spectra at various temperatures with an interval of ≈ 100 K (measurements were performed at every 50 K in practice, though not all are shown here). The saturation of the T dependence was observed at the respective highest T (presented with light gray lines), except for $x=0.33$ (>290 K) and $x=0.5$ (>540 K). For $x=0.7$, we confirmed that the saturation occurs around 340 K by reflectivity measurements between 0.08 and 0.8 eV (not shown in the figure). The original reflectivity spectra for the respective x are shown in the left side of Fig. 6. Several peak structures observed below 0.1 eV are due to optical phonon modes. The observed reflectivity spectra for all x are strongly dependent on T in a wide energy region, reflecting the evolution of charge correlation with lowering T. At high T, all the spectra show comparatively similar features with appreciable spectral weight below 0.5 eV and well-screened phonon structures. As x is increased above 0.5, however, the spectral feature becomes more metal-like and less T dependent. In the optical conductivity spectra (the right panel of Fig. 6), which

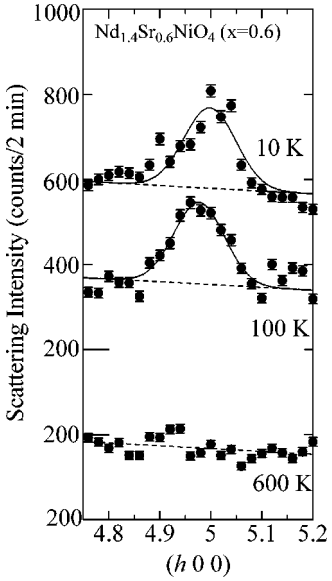

FIG. 7. Temperature variation of the superlattice peak profile at around (5 0 0) indicative of the checkerboard-type charge order. The scanning direction is along (h 0 0). The solid lines are results of a Gaussian curve fitting, whereas the h-linear broken lines indicate the scattering intensity from the background.

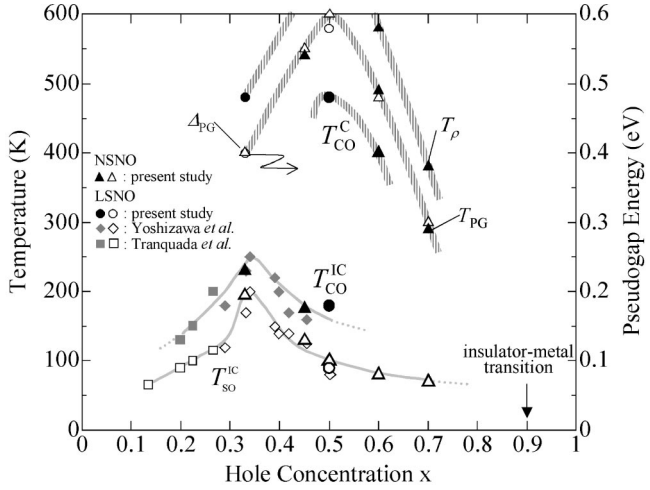

FIG. 8. The electronic phase diagram of $R_{2-x}Sr_xNiO_4$ (R=La and Nd). Transition temperatures of stripe charge order (T^{IC}_{CO}), stripe spin order (T^{IC}_{SO}), and checkerboard (CB) charge order (T^{C}_{CO}), observed by neutron diffraction measurements, are plotted as functions of x together with the onset temperatures of pseudogap formation (T_{PG}) and the resistivity upturn temperature ($T_{\rho_{ab}}$). The energy of the pseudogap (Δ_{PG}), as defined by the isosbectic point of the optical conductivity spectra (see Fig. 6), is also plotted with the scale on the right coordinate. The triangle (circle) marks represent the results for NSNO (LSNO) in the present study. The curves in the diagram are merely a guide for the eyes.

were transformed by Kramers-Kronig analysis, qualitatively similar T-dependent behaviors are observed for all x, as already discussed for $x=0.5$. The isosbectic point at $T>T_{CO}$, defined as Δ_{PG} in Sec. III A, shows a clear x dependence. The Δ_{PG} values (indicated by arrows in Fig. 6) are 0.4 eV for $x=0.33$, 0.55 eV for 0.45, 0.60 eV for 0.50, 0.48 eV for 0.60, and 0.30 eV for 0.70. The Δ_{PG} provides an estimate of energy scale of charge correlation between doped holes. As for the temperature scale, the onset temperature of pseudogap formation T_{PG} is estimated within an uncertainty of 50 K as the temperature where saturation of T dependence is observed. The T_{PG} values thus estimated are 540 K for $x=0.45$, >540 K for 0.50, 490 K for 0.60, and 290 K for 0.70, respectively. Both Δ_{PG} and T_{PG} reach a maximum at $x=0.5$, indicating that the strongest charge correlation takes place at this half-doped state.

In Fig. 5(a), the T dependence of the neutron-diffraction superlattice peak (5 0 0) intensity normalized by a standard Bragg reflection is plotted for R=Nd and $x=0.6$ and 0.7. In Fig. 7, we exemplify the T-variation of the peak profile along (h 0 0) at $h\sim5$ for $x=0.6$. At 10 and 100 K, diffusive peak at $h\approx5$ can be distinguished, while at 600 K the peak disappears and only the flat background is observed. This superlattice peak is characteristic of the CB-type charge order, as described in Sec. III A. The solid lines are Gaussian fitted curves whereas the h-linear broken lines indicate the scattered intensity from the background. In Fig. 5(a), the T variation of the background intensity measured at (4.7 0 0) has been subtracted for the respective samples. For $x=0.7$, the (5 0 0) peak exists but is so weak and diffusive that we can only show its intensity at 10 K with an appreciable error bar.

In Figs. 5(b) and 5(c) we present the spectral weight change ΔN_{eff} estimated with the same procedure as described in the previous section and the frequency of Ni-O bending phonon mode for $0.5\leqslant x\leqslant0.7$, respectively. At the first glance, the very similar relation as discussed for $x=0.5$ also stands for $x=0.6$ and 0.7. The onset temperature of phonon mode splitting decreases from 450 K ($x=0.5$) or 400 K ($x=0.6$) to 150 K ($x=0.7$) as the CB-type charge order parameter diminishes with x. On the other hand, ΔN_{eff} is closely correlated with the CB-type charge order superlattice peak intensity for both T- and x-dependence. To be exact, ΔN_{eff} is more enhanced in a high-T and high-x region than the superlattice peak intensity, which must be due to its finer sensitivity to the dynamical component of charge order. The charge correlation, which manifests itself as the opening of pseudogap and suppresses coherent hole motion, is thus assigned to the CB-type charge order fluctuation in $0.5\leqslant x\leqslant0.7$.

To summarize the results mentioned above, the overall phase diagram is presented in Fig. 8. From the results of neutron diffraction, we can conclude the variation of the ground state as follows: In $x\leqslant0.45$, the stripe order with $\epsilon\sim x$ subsists, while no clear evidence for the CB-order is observed. For $x\geqslant0.5$, on the other hand, the CB-type charge ordered phase seems to coexist with the stripe phase whose incommensurability ($\epsilon\approx0.44$) is nearly independent of x.[16] As for the transition temperatures of stripe order, T^{IC}_{CO} and T^{IC}_{SO} rise with x to take a maximum at $x=1/3$ with 240 and 180 K, respectively, and then turn to decrease monotonically with further doping. However, the spin stripe order is observed up to $x=0.7$, indicating the robustness of spin interaction. The CB-type charge order, on the other hand, abruptly appears at $x=0.5$ at such a high temperature as $T^{C}_{CO}\sim480$ K. As further increasing x, T^{C}_{CO} rapidly decreases

to ~400 K for $x=0.6$, and for $x=0.7$ the superlattice diffraction becomes diffusive and barely discerned at low T. Thus, the clear difference in the T scale and x dependence indicates that the stripe and the CB-type order must be different in origin, as already argued in Sec. III A. The reason why the order pattern in $x \geqslant 0.5$ is x independent might be that the excess holes tend to reside in the $3z^2-r^2$ orbital state. This is supported by the fact that the c-axis length takes the maximum at $x=0.5$ and tends to decrease with increasing x above $x=0.5$, as shown in Fig. 1. This suggests a decrease (increase) of the $3z^2-r^2$ electron (hole) count. The increase of the $3z^2-r^2$ hole count is also evidenced by the gradual evolution of in-gap state in c-axis $\sigma(\omega)$ which was observed by absorption measurements of LSNO thin films in a high-doped ($x>0.5$) region.[11,26] Furthermore, a similar behavior has also been reported for the so-called CE-type spin-charge-orbital order in $Pr_{1-x}Ca_xMnO_3$. In this case, a commensurate charge order similar to the CB-type order in RSNO takes place at $0.3<x<0.5$.[27] Its x-independent order pattern in a wide doping region can be attributed to the occupancy of $3z^2-r^2$ orbital by excess *electrons*, which was confirmed by electron diffraction measurement.[28] Thus, the present case in RSNO may be regarded as the *hole* counterpart.

The onset temperature of resistivity upturn ($T_{\rho_{ab}}$), that of pseudogap formation (T_{PG}), and the pseudogap energy (Δ_{PG}) are also plotted in Fig. 8. These quantities can give a good estimate of the energy scale of the charge correlation that suppresses the coherent motion of holes. They seem to be correlated with each other, taking a broad maximum at $x=0.5$. This indicates that the correlation among doped holes becomes the strongest at $x=0.5$ by taking a form of the CB type. With the increase of x above 0.5, on the other hand, $T_{\rho_{ab}}$, T_{PG}, and Δ_{PG} monotonically decrease as the CB-type order is weakened. It would be interesting to compare the present results with transport and optical properties of LSNO investigated recently using single-crystalline thin films in $0.5 \leqslant x \leqslant 1.4$.[11,12] According to the results on the thin films, a nondiverging resistivity was at first observed at $x \sim 0.9$ which is viewed as the critical point of the insulator-metal (I-M) transition. In $x<0.9$, a similar pseudogap behavior was observed in the in-plane $\sigma(\omega)$ spectra. The energy scale of the pseudogap, Δ_{PG}, also similarly decreases as x is increased, and eventually becomes undetectable at around $x_{\mathrm{I\text{-}M}}=0.9$, crossing the lower-$\omega$ limit (≈ 0.2 eV) of the thin-film measurement. In $0.9 \leqslant x < 1.2$, however, $\sigma(\omega)$ still shows the T dependence indicative of pseudogap formation, and the resistivity upturn and T-dependent Hall coefficient are also observed. They all have been attributed to remnant charge/spin ordering correlation.[12] Taking the nearly parallel behaviors between LSNO and NSNO in the pre-transition region ($0.5 \leqslant x \leqslant 0.7$) into account, the I-M transition in LSNO (Refs. 11 and 12) is likely attributed to the melting of the CB-type charge order.

IV. SUMMARY

We have performed neutron diffraction and optical studies on the charge ordering and related charge dynamics in $La_{2-x}Sr_xNiO_4$ ($x=0.5$) and $Nd_{2-x}Sr_xNiO_4$ ($0.33 \leqslant x \leqslant 0.7$) systems. We found that a commensurate checkerboard (CB)-type charge order abruptly emerges at $x \geqslant 0.5$. In addition, an incommensurate stripe order was observed to subsist up to $x=0.7$, where modulation vector and ordering temperatures change continuously in the lower-doped region and then saturate for $x \gtrsim 0.45$. These results indicate that there are two different kinds of ordering processes in this system, which coexist and compete with each other as the low-temperature state. The in-plane resistivity upturn and the pseudogap formation in the optical conductivity spectrum seem to reflect the evolution of the CB-type charge order correlation, whose temperature scale takes a local maximum at $x=0.5$. The transition temperature of the CB-type charge order could also be detected as the splitting of the specific infrared phonon mode. The amplitude and the temperature and energy scales of the pseudogap monotonically decrease as x increases from 0.5 to 0.7, similar to the decrease of the amplitude and transition temperature of the CB-type charge order. These results suggest that I-M transition around $x \sim 0.9$ in this system may occur concomitantly with the disappearance of the CB-type charge order.

ACKNOWLEDGMENTS

The authors thank K. Chatani and K. Hirota for the rent of the wide-T cryostat for the high temperature neutron diffraction measurements. Some of the authors (K. I. and R. K.) were supported by the Japan Society for the Promotion of Science for Young Scientists. This work was partly supported by Grant-In-Aids for Scientific Research from the Ministry of Education, Culture, Sports, Science, and Technology, Japan.

*Present address: Institute for Materials Research, Tohoku University, Sendai 980-8577, Japan.

[1] M. Imada, A. Fujimori, and Y. Tokura, Rev. Mod. Phys. **70**, 1039 (1998).

[2] For a review, J. Zaanen, Science **286**, 251 (1999), and references cited therein.

[3] M. Fujita, K. Yamada, H. Hiraka, P. M. Gehring, S. H. Lee, S. Wakimoto, and G. Shirane, Phys. Rev. B **65**, 064505 (2002).

[4] C. H. Chen, S.-W. Cheong, and A. S. Cooper, Phys. Rev. Lett. **71**, 2461 (1993).

[5] V. Sachan, D. J. Buttrey, J. M. Tranquada, J. E. Lorenzo, and G. Shirane, Phys. Rev. B **51**, 12 742 (1995).

[6] J. M. Tranquada, J. E. Lorenzo, D. J. Buttrey, and V. Sachan, Phys. Rev. B **52**, 3581 (1995).

[7] J. M. Tranquada, D. J. Buttrey, and V. Sachan, Phys. Rev. B **54**, 12 318 (1996).

[8] P. Wochner, J. M. Tranquada, D. J. Buttrey, and V. Sachan, Phys. Rev. B **57**, 1066 (1998).

[9] H. Yoshizawa, T. Kakeshita, R. Kajimoto, T. Tanabe, T. Katsufuji, and Y. Tokura, Phys. Rev. B **61**, R854 (2000).

[10] R. J. Cava, B. Batlogg, T. T. Palstra, J. J. Krajewski, W. F. Peck, Jr., A. P. Ramirez, and L. W. Rupp, Jr., Phys. Rev. B **43**, 1229 (1991).
[11] S. Shinomori, M. Kawasaki, and Y. Tokura, Appl. Phys. Lett. **80**, 574 (2002).
[12] S. Shinomori, Y. Okimoto, M. Kawasaki, and Y. Tokura, J. Phys. Soc. Jpn. **71**, 705 (2002).
[13] S.-W. Cheong, H. Y. Hwang, C. H. Chen, B. Batlogg, L. W. Rupp, Jr., and S. A. Carter, Phys. Rev. B **49**, 7088 (1994).
[14] T. Katsufuji, T. Tanabe, T. Ishikawa, S. Yamanouchi, Y. Tokura, T. Kakeshita, R. Kajimoto, and H. Yoshizawa, Phys. Rev. B **60**, R5097 (1999).
[15] A. P. Ramirez, P. L. Gammel, S.-W. Cheong, D. J. Bishop, and P. Chandra, Phys. Rev. Lett. **76**, 447 (1996).
[16] R. Kajimoto, K. Ishizaka, H. Yoshizawa, and Y. Tokura, Phys. Rev. B **67**, 014511 (2003).
[17] K. Sugiyama, H. Nozaki, T. Takeuchi, and H. Ikuta, J. Phys. Chem. Solids **63**, 979 (2002).
[18] T. Katsufuji, T. Tanabe, T. Ishikawa, Y. Fukuda, T. Arima, and Y. Tokura, Phys. Rev. B **54**, R14 230 (1996).
[19] K. Yamamoto, K. Ishizaka, E. Saitoh, S. Shinomori, T. Tanabe, T. Katsufuji, and Y. Tokura, Phys. Rev. B **67**, 014414 (2003).
[20] K. Yamamoto, T. Katsufuji, T. Tanabe, and Y. Tokura, Phys. Rev. Lett. **80**, 1493 (1998).
[21] G. Blumberg, M. V. Klein, and S.-W. Cheong, Phys. Rev. Lett. **80**, 564 (1998).
[22] The reduction of gap at low T was also reported by Jung *et al.* (Ref. 23), together with simultaneous re-expansion of the a-axis length. It may be attributed to the excess holes occupying the $3z^2-r^2$ orbital state. Note that the $\epsilon \sim 0.44$ stripe requires only 0.44 holes/Ni, whereas 0.50 holes/Ni is necessary for the CB-type ordered state.
[23] J. H. Jung, D.-W. Kim, T. W. Noh, H. C. Kim, H.-C. Ri, S. J. Levett, M. R. Lees, D. McK. Paul, and G. Balakrishnan, Phys. Rev. B **64**, 165106 (2001).
[24] The spin stripe correlation is well developed at somewhat higher temperature than T_{SO}^{IC}: In a recent inelastic neutron scattering study in LSNO ($x=0.275$), the incommensurate magnetic fluctuation was observed already at room temperature (Ref. 25). An abrupt reduction in damping energy of fluctuation was observed as lowering T through the charge order transition, which may be prerequisite for the magnetic ordering.
[25] S.-H. Lee, J. M. Tranquada, K. Yamada, D. J. Buttrey, Q. Li, and S.-W. Cheong, Phys. Rev. Lett. **88**, 126401 (2002).
[26] S. Shinomori, Ph.D. thesis, University of Tokyo, 2001.
[27] Z. Jirak, S. Krupicka, Z. Simsa, M. Dlouha, and S. Vratislav, J. Magn. Magn. Mater. **53**, 153 (1985).
[28] T. Asaka, S. Yamada, S. Tsutsumi, C. Tsuruta, K. Kimoto, T. Arima, and Y. Matsui, Phys. Rev. Lett. **88**, 097201 (2002).